Available online at www.sciencedirect.com
ScienceDirect
Journal of Contaminant Hydrology 92 (2007) 255–273
JOURNAL OF Contaminant Hydrology
www.elsevier.com/locate/jconhyd

Bacteria transport and deposition under unsaturated conditions: The role of the matrix grain size and the bacteria surface protein

G. Gargiulo [a,*], S. Bradford [b], J. Šimůnek [c], P. Ustohal [a], H. Vereecken [a], E. Klumpp [a]

[a] *Agrosphere (ICG-IV), Institute of Chemistry and Dynamics of the Geosphere (ICG), Forschungszentrum, Jülich GmbH D-52425, Jülich, Germany*
[b] *USDA-ARS, George E. Brown, Jr. Salinity Laboratory, 450 W. Big Springs Road, Riverside, CA 92507–4617, United States*
[c] *Department of Environmental Sciences, University of California, Riverside, CA 92521, United States*

Received 28 April 2006; received in revised form 31 October 2006; accepted 3 January 2007
Available online 24 January 2007

Abstract

Unsaturated (80% water saturated) packed column experiments were conducted to investigate the influence of grain size distribution and bacteria surface macromolecules on bacteria (*Rhodococcus rhodochrous*) transport and deposition mechanisms. Three sizes of silica sands were used in these transport experiments, and their median grain sizes were 607, 567, and 330 μm. The amount of retained bacteria increased with decreasing sand size, and most of the deposited bacteria were found adjacent to the column inlet. The deposition profiles were not consistent with predictions based on classical filtration theory. The experimental data could be accurately characterized using a mathematical model that accounted for first-order attachment, detachment, and time and depth-dependent straining processes. Visual observations of the bacteria deposition as well as mathematical modelling indicated that straining was the dominant mechanism of deposition in these sands (78–99.6% of the deposited bacteria), which may have been enhanced due to the tendency of this bacterium to form aggregates. An additional unsaturated experiment was conducted to better deduce the role of bacteria surface macromolecules on attachment and straining processes. In this case, the bacteria surface was treated using a proteolitic enzyme. This technique was assessed by examining the Fourier-transform infrared spectrum and hydrophobicity of untreated and enzyme treated cells. Both of these analytical procedures demonstrated that this enzymatic treatment removed the surface proteins and/or associated macromolecules. Transport and

* Corresponding author.
E-mail address: grazgar@yahoo.it (G. Gargiulo).

doi:10.1016/j.jconhyd.2007.01.009

modelling studies conducted with the enzyme treated bacteria, revealed a decrease in attachment, but that straining was not significantly affected by this treatment.

Keywords: Bacteria transport; Classical filtration theory; Unsaturated flow; *Rhodococcus rhodochrous*

1. Introduction

Microbial contamination of groundwater is a serious problem that can result in large outbreaks of waterborne disease (Fontes et al., 1991; Scandura and Sobsey, 1997; Ginn et al., 2002; Reynolds et al., 2004). Most waterborne pathogens (viruses, bacteria, and protozoan parasites) are of faecal origin, and come from either human and/or animal wastes. These solid wastes (biosolids and manure) and contaminated effluents from wastewater treatment plants and concentrated animal feeding operations are frequently land applied as a means of treatment and/or disposal. An ability to accurately predict the transport and fate of pathogenic microorganisms in unsaturated soil environments is therefore needed to protect surface and groundwater resources from contamination. On the other hand, many bacteria can beneficially degrade or immobilize environmental contaminants (Grasso et al., 1996; Schaefer et al., 1998; Bolster et al., 2001; Ginn et al., 2002). Bioremediation and/or bio-augmentation strategies to clean up recalcitrant chemicals in subsurface environments could be greatly enhanced by efficient delivery of specialized bacteria to targeted locations in the subsurface.

In comparison to saturated systems, relatively few studies have examined the transport and deposition behaviour of bacteria under unsaturated condition (Wan et al., 1994; Powelson and Mills, 1996; Schafer et al., 1998; Jewett et al., 1998; Gargiulo et al., submitted for publication). Mechanisms of microbe deposition in unsaturated porous media include attachment, interfacial attachment, straining, and film straining. Attachment and interfacial attachment refers to deposition on the solid–water and air–water interface, respectively. Conversely, microbe deposition by straining and film straining occurs due to physical restrictions of the pore geometry and the water film thickness, respectively. Both attachment and straining processes are expected to be functions of colloid–colloid, colloid–solvent, colloid–interface interactions and system hydrodynamics that will influence mass transfer and fixation at locations of deposition. It should be noted, however, that the bulk of the research on colloid transport have focused on attachment, and have not considered the potential influence of pore geometry on deposition.

In contrast to abiotic colloids, bacteria surfaces have a more complicated chemical structure. The bacteria surface layers (S-layers) are the outer components of the cell wall and consist primarily of proteins. The rate and the extent of bacteria attachment to soil surfaces and air–water interfaces are governed by molecular-scale interactions between the bacteria outer layer and a particular interface. Since the surface macromolecular structure is not well known, these interactions are poorly understood, in particular the role of cell surface polymers (Caccavo, 1999). These macromolecules can inhibit or promote attachment in accordance with their affinities for the interface and depending on the aqueous solution chemistry (Salerno et al., 2004).

Classical filtration theory (CFT) predicts that the deposition profile of attached colloids will decrease exponentially with increasing transport depth. Recent experimental studies, however, have reported that CFT is frequently inadequate to describe colloid and bacteria deposition profiles when a energy barrier exists (unfavourable deposition conditions), and for larger sized

colloids and finer textured media (DeFlaun et al., 1997; Bolster et al., 2001; Bradford et al., 2002, 2003; Tufenkji et al., 2004; Tufenkji and Elimelech, 2004; Johnson et al., 2005; Bradford and Bettahar, 2005, 2006; Gargiulo et al., submitted for publication). For unfavourable conditions, the deposition profile has frequently been reported to follow a hyper-exponential (power law) distribution, implying a decreasing rate of deposition with transport distance (Bradford et al., 2006). Different hypotheses have been formulated and reported in the literature to account for these experimental observations. Chemical explanations that have been proposed include: porous media charge variability (Johnson and Elimelech, 1995), heterogeneity in the surface charge of the colloids (Bolster et al., 2001); and colloid deposition in the secondary energy minimum of the Derjaguin-Landau-Verwey-Overbeek (DLVO) potential energy distribution (Li et al., 2004; Tufenkji and Elimelech, 2005a,b). Other authors have presented an explanation based on pore structure. For example, Bradford et al. (2002, 2003), Tufenkji et al. (2003), and Foppen et al. (2004) related the deviations from CFT predictions to straining.

The aim of this work is to improve our understanding of bacteria deposition mechanisms in unsaturated conditions. Specifically, we attempt to better quantify the roles of attachment and straining processes. A set of unsaturated column experiments was performed using various sized sands. Straining has previously been reported to increase with decreasing sand size in saturated porous media McDowell-Boyer et al., 1986; Bradford et al., 2002, 2003) and decreasing water saturation in unsaturated systems (Gargiulo et al., submitted for publication). The coupled role of water saturation and grain size on straining deposition, however, has not yet been systematically studied. A proteolitic enzymatic treatment was employed to investigate the role of surface proteins on bacteria attachment. This technique also proved to be a useful tool to discriminate straining and attachment deposition processes. Data analysis of the breakthrough curves and deposition profiles was further aided by using fitted model parameters that accounts for time-dependent attachment and/or straining processes.

2. Materials and methods

2.1. Bacteria

The bacterial strain *Rhodococcus rhodochrous* (DSMZ 11097) was used in the unsaturated transport experiments. *R. rhodochrous* is a gram-positive spherical bacterium of 1 μm that is able to form big three-dimensional aggregates as large as 10–15 μm. This strain was isolated from soil contaminated with alkenes by Kästner (1989). Rhodococci are aerobic actinomycetes that exhibit a diverse range of metabolic activities. Rhodococci have the ability to degrade hydrocarbon chains and a variety of organic compounds, including xenobiotic compounds like PCB and benzothiophene.

R. rhodochrous was grown on agar plates consisting of ATCC Medium 220: CASO AGAR (Merck 105458), peptone from casein (15.0 g), peptone from soy meal (5.0 g), NaCl (5.0 g), agar (15.0 g), and distilled water (1000 ml). For column experiments, this bacterial strain was cultivated at 30 °C in a nutrient broth that was agitated at 130 rpm using a thermo stated shaker (*Certomax HK BRAUN*®). The nutrient broth consisted of mineral medium (Brunner) Na_2HPO_4 (2.44 g), KH_2PO_4 (1.52 g), $(NH_4)_2SO_4$ (0.50 g), $MgSO_4 \times 7\ H_2O$ (0.20 g), $CaCl_2 \times 2\ H_2O$ (0.05 g), trace element sol. (10 ml), glucose (5.0 g), and distilled water (1000 ml). The bacteria cells were harvested from the nutrient broth in the late stationary phase by gentle centrifugation (10 min, 8000 rpm, 25 °C) and re-suspended in phosphate buffer saline 10^{-4} M, pH = 7. In this

phase the substrate had been consumed, the cell culture stopped growing, and the cells had reached a resting mode.

Gargiulo et al. (submitted for publication) previously reported information on the surface characteristics and morphology of *R. rhodochrous*. This information is briefly summarized below. The hydrophobicity of *R. rhodochrous* was quantified using the M.A.T.H. approach (microbial adhesion to hydrocarbon). Between 55 to 90% of the bacteria partitioning to the hydrocarbon-water interface, indicating that it is very hydrophobic. The zeta potential was measured at 25 °C using a suspension of $7*10^8$ cells per ml (phosphate buffer 10^{-4} M pH=7) and a Lazer Zee Meter (Pen Kem, Model 501) equipped with a video system to be -47 ± 7 mV. An epifluorescent microscope was used to determine the morphology of *R. rhodochrou*s. This bacterium exhibits three-dimensional aggregates that can reach the size of 10–15 μm, while single cells have a diameter of only 0.8–1 μm.

Some of the bacteria cells of *R. rhodochrous* were harvested and treated by a proteolitic enzyme to remove the proteins and associated macromolecules on the surface of the cells that may promote attachment to solid substrates. The harvested cells were then re-suspended in Chymotrypsin solution (100 U/ml) consisting of 350 U/mg of Chymotrypsin powder (Sigma) and a solution of 100 U/ml in Tris HCl buffer (0.1 M and pH=7). The Tris HCl buffer was prepared using 12.1 g of Trizma base that was diluted in 1 l of deionized and sterile water, and 4.1 ml of 30% HCl. The cells and solution were left in the dark at 37 °C for 2 h and agitated at 130 rpm using a thermo stated shaker (*Certomax HK BRAUN*®). The bacteria cells were then washed twice with a 10^{-4} M (pH=7) phosphate buffer saline solution.

The infrared (IR) spectra of the untreated and treated bacterial cell samples were recorded using a BRUKER EQUINOX model 55/S (OPUS software version 5.5) Fourier-transform (FT) spectrometer to quantify the effect of proteolitic enzymatic treatment on the surface properties of *R. rhodochrous*. The bacteria cells were harvested during late stationary phase by centrifugation (1000 rpm for 2 min, 25 °C) and cell pellets were obtained. The bacteria were washed twice with phosphate buffer solution (10^{-4} M and pH=7) and re-pelleted by centrifugation at 1000 rpm for 2 min. The pellets were scraped on ATR (ZnSe)-crystal for reflection (which are highly transparent to IR radiation) with a sterile bacteriological loop and air dried for 15 min at room temperature (or for 5 min by air drying in a laminar flow hood). FT-IR measurements were performed in the transmission mode with a liquid-nitrogen-cooled MCT detector that was connected to the FT-IR microscope (Bruker IRScope II) and spectrometer. The spectra were obtained over the wave number range of 600–4000 nm. Typical measurement times while recording the spectra were about 4 min (60 scan) at a resolution of 4 nm. For each sample, the spectrum was taken as the average of five measurements. There were no significant differences (SD) in the spectra from the various sites (SD did not exceed 0.005). The aperture that was used in this study and that provided the best signal/noise ratio was 100 μm.

2.2. Porous media

Three different sands were used in the transport experiments. These sands consisted of several sieve sizes of sterile fused silica sand (*Teco-Sil, C-E Minerals Greenville, USA*). The grain size distribution of the various sands was determined by sieve analysis (*Laser Particle Sizer Fritsch analysette 22*). The median grain size of the three sands was 607, 567, and 330 μm. The coefficient of uniformity for the 607, 567, and 330 μm sand was 1.44, 1.87, and 1.81, respectively.

2.3. Packed column experiments

Gargiulo et al. (submitted for publication) previously reported on the setup that was used in the packed column experiments. Only an abbreviated discussion is provided below. The experimental column (diameter 8.0 cm and length 22.5 cm) was constructed from Plexiglas and consisted of 4 filled sections (5 cm in length) and one empty section (2.5 cm in length). The column was provided with pressure probes (*tensiometer* with *PMP 4070 pressure transducers*) near the top and near the bottom to verify unit gradient conditions. The air phase in the column was maintained at atmospheric pressure by means of two aeration openings. At the top of the column a sprinkling plate equipped with 80 stainless steel needles was used to evenly distribute the influent over the sand surface at a rate of 165–170 ml/h. The water and the solution were supplied to the sprinkling plate using a piston pump (*Ismatec Reglo CPF*). The bottom was formed by a porous stainless steel plate covered with a hydrophilic membrane (polyester fabric, mesh size 15 μm). The suction at the bottom of the column was adjusted to achieve unit gradient by adjusting the drip point of a hanging water column. Steady-state water flow conditions were kept constant for the remainder of the transport experiment. The total column water content was continuously monitored gravimetrically using a digital balance (*Sartorius® CP12001S*). The column bottom was connected with PVC tubes (2 mm inner diameter) to a conductivity probe (WTW *D823662 Heilheim LDM/S)*, spectrophometer (*Tidas Spectralitic*) and UV detector (*Hitachi-Merck f-1050*), respectively. Both the bacteria and the tracer outflow concentration were monitored on-line.

The column was uniformly packed with dry sand. The porosity of the packing was determined gravimetrically (*Sartorius® CP12001S digital balance*). Water was introduced into the column by slowly pumping upwards at a constant rate until a water saturation of approximately 80% (containing residual entrapped air bubbles) was achieved. Unit gradient conditions were then obtained following the protocol outlined above. Before initiating the transport experiment, the sand pack was equilibrated by flushing it with several pore volumes of phosphate buffer solution (pH=7 and 10^{-4} M).

The final spatial distribution of retained bacteria was measured following each transport experiment according to the procedure described by Gargiulo et al. (submitted for publication). The deposition profile of retained cells per gram of dry sand was determined from measured values of the total organic carbon content (TOC) in the sand. Experimental mass balance was calculated independently for the cells in the effluent and retained cells, and normalized by the total number injected into the column.

2.4. Theory and model

The experimental data were characterized using the HYDRUS-1D code (Šimůnek et al., 2005). Relevant aspects of the code are briefly summarized below. The code numerically solves the *Richards* equation for saturated–unsaturated water flow. The bacteria transport was modelled using a modified form of the convection–dispersion equation, in which kinetic adsorption sites were considered for both attachment (s_1) and straining (s_2) processes. The mass balance equation is defined as:

$$\frac{\partial \theta c}{\partial t} + \rho_b \frac{\partial s}{\partial t} = \frac{\partial}{\partial x}\left(\theta D \frac{\partial c}{\partial x}\right) - \frac{\partial qc}{\partial x} \tag{1}$$

where θ is the volumetric water content, ρ_b is the soil bulk density [ML^{-3}], t is the time [T], q is the flow rate [LT^{-1}], x is the spatial coordinate [L], D is the dispersion coefficient [L^2T^{-1}], c is

the bacteria concentration in the aqueous phase [N_cL^{-3}], s is the solid phase concentration [N_cM^{-1}], and N_C is the number of bacteria. The classical filtration theory (CFT) assumes that the mass transfer between the aqueous and solid phase can be described as:

$$\rho\frac{\partial s}{\partial t} = \theta\psi_t k_a c - k_d\rho_b s \tag{2}$$

where k_a is the first-order attachment coefficient [T^{-1}], k_d is the first-order detachment coefficient [T^{-1}], and ψ_t is a dimensionless colloid retention function that accounts for time-dependent deposition. To simulate reductions in the time-dependent deposition coefficient due to the blocking or filling of favourable deposition sites, ψ_t is sometimes assumed to decrease with increasing colloid mass retention. A Langmuirian dynamics (Adamczyk et al., 1994) equation has been proposed for ψ to describe this phenomenon as:

$$\psi_t = 1-\frac{s}{s_{max}} \tag{3}$$

in which s_{max} is the maximum solid phase concentration [N_cM^{-1}] of colloids on sorption sites.

Several studies (e.g., Schijven and Šimůnek, 2002; Bradford et al., 2002, 2003) divided sorption sites into two fractions ($s=s_1+s_2$) and assumed different rates or processes occurring at each sorption site. Eq. (2) can then be rewritten as follows (Bradford et al., 2003):

$$\rho\frac{\partial s}{\partial t} = \rho\frac{\partial(s_1+s_2)}{\partial t} = \theta\psi_t k_a c - k_d\rho_b s_1 + \theta k_{str}\psi_x c \tag{4}$$

where k_{str} is the first-order straining coefficient [T^{-1}], and coefficients ψ_t and ψ_{str} are dimensionless colloid retention functions that account for time and/or depth-dependent deposition. Note that the detachment process occurs only from the first sorption sites. In this analysis, attachment to the solid phase and the air–water interface can be lumped in the k_a term. Similarly, straining in pores and water films are also considered to be lumped using the k_{str} term.

Bradford et al. (2003) hypothesized that the influence of depth-dependent straining processes on colloid retention can be described using the following coefficient:

$$\psi_x = \left(\frac{d_c + x - x_0}{d_c}\right)^{-\beta} \tag{5}$$

where d_c is the median diameter of the sand grains [L], x_0 is the coordinate [L] of the location where the straining process starts (in this case the surface of the soil profile), and β is an empirical factor controlling the shape of the spatial distribution. In this work, when we consider both time and depth-dependent straining, the value of colloid retention function in the straining term of Eq. (4) is equal to the product of ψ_t and ψ_x.

In the Results and discussion section below, we will refer to model fits based on Eqs. (1) and (2) with $\psi=1$ (i.e., without blocking) as the CFT model and with $\psi\leq 1$ (i.e., with blocking of favourable deposition sites) as the Langmuirian blocking model. Model fits based on Eqs. (1) and (4) will be referred to as the Straining model. The code allowed us to fit simultaneously the parameters k_a, k_d, k_{str}, s_{max} and β, while considering both the breakthrough curve and the retention profile in the parameter optimisation. The mean pore water velocity and dispersivity were obtained by fitting the solution of the convective dispersion equation for the tracer breakthrough curve.

3. Results and discussion

3.1. Role of grain size

Fig. 1A presents the breakthrough curves for *R. rhodochrous* using 330, 567 and 607 μm sands when the water saturation was 80%. Here the relative effluent concentration, c/c_0, is plotted as a function of pore volume. The bacteria breakthrough curves always coincide with the arrival of a conservative tracer (data not shown). The comparison of the effluent concentrations in Fig. 1A indicates that the sand size plays a significant role in the bacteria transport and deposition under unsaturated conditions. The effluent concentration of cells decreased with decreasing grain size. The peak effluent concentration was 0.92, 0.7, and 0.02 for the 607, 567, and 330 μm sands, respectively. Effluent mass balance information provided in Table 1 also supports this finding. Fontes et al. (1991) also found a similar effect of sand size on bacteria transport under saturated condition. These authors attributed this behaviour to the larger average pore diameter in coarser sands.

Fig. 1B shows the corresponding bacteria deposition profiles for the variously sized sands when the water saturation was 80%. The amount of bacteria that was retained in the sand

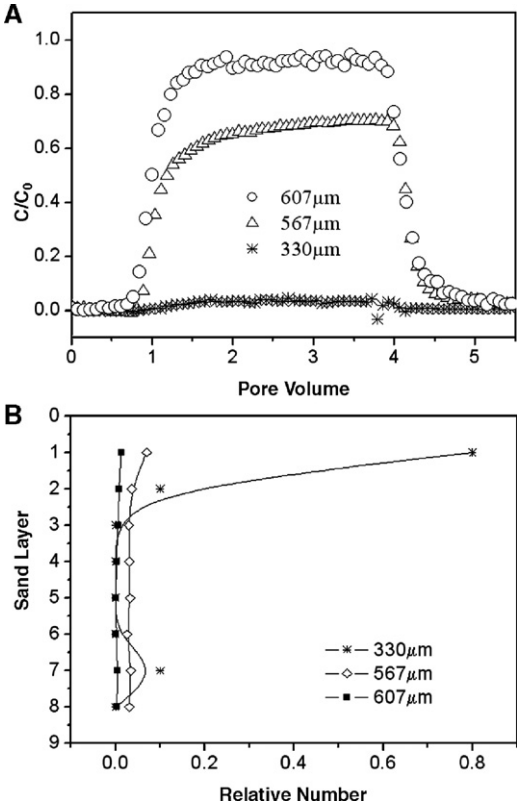

Fig. 1. *Rhodococcus rhodochrous* transport experiment under unsaturated conditions (80%) with different sand grain sizes. (A) Breakthrough curves. (B) Retention profiles expressed using relative numbers, i.e., the number of bacteria found in each soil layer divided by the total number of bacteria injected.

Table 1
Experimental and modelled mass balances for *Rhodococcus rhodochrous* cells in the column outflow and retained in the column

Grain size	Experimental		Modeled		
	% Outflow	% Retained	% Attached	% Strained	Total % retained
Coarse sand	95	7	0.9	9.7	10.6
Medium sand untreated cells	63	33	7.8	27.6	35.4
Medium sand treated cells	72	17	3.4	17.6	20.9
Fine sand	5	98	0.4	96.7	97.1

The straining model was used in calculations.

increased with decreasing sand size. All of the deposition profiles were hyper-exponential and tended to decrease monotonically with distance from the injection point. Retained concentrations were highest near the column inlet, especially for decreasing sand sizes. In the finest grain size sand (330 μm) nearly all the bacteria (97%) were retained adjacent to the column inlet.

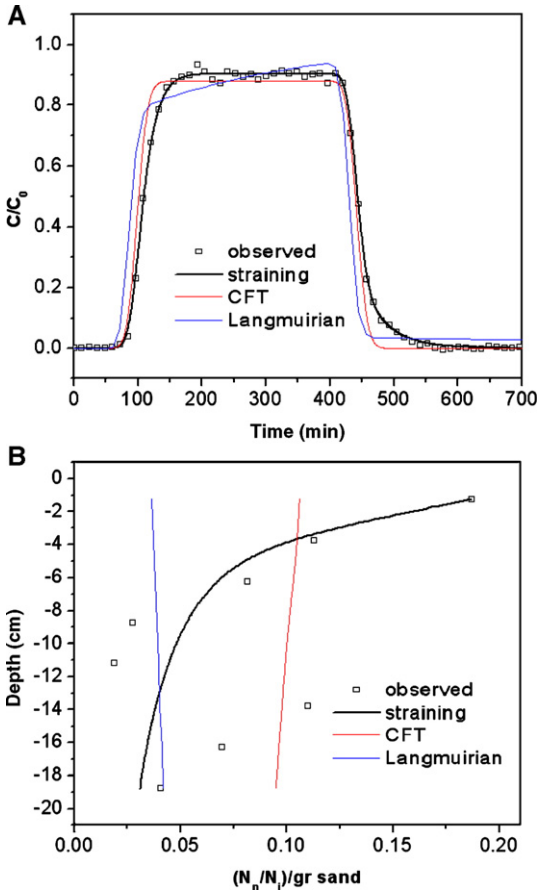

Fig. 2. Measured and fitted breakthrough curves (A) and retention profiles (B) for untreated *Rhodococcus rhodochrous* at 80% saturation and grain size of 607 μm. Fitted curves were obtained using the classical filtration theory (CFT) (red), Langmuirian blocking (blue), and straining (black) models.

The effluent and spatial distribution data presented in Fig. 1A and B, respectively, were simulated using the CFT and Langmuirian blocking models to better deduce mechanism of deposition. Simulation results are shown in Figs. 2, 3 and 4 for the 607, 567, and 330 μm sands, respectively. Table 2 summarizes fitted model parameters as well as statistical parameters for the goodness of fit. Note in Figs. 2–4 and Table 2 that the CFT and the Langmuirian blocking provide an adequate description of the breakthrough curves, but a much poorer characterization of the deposition profiles. The sticking efficiency for the CFT model was calculated from the fitted values of k_a and predicted values of the collector efficiency (Tufenkji and Elimelech, 2004). Values of the sticking efficiency (α) are theoretically independent of the grain size of the sand and should only dependent on the chemistry of the colloids, aqueous phase, and porous media. Calculated values of the sticking efficiency, however, systematically increased with decreasing sand size, with α equal to 0.018, 0.05, and 0.568 for 607, 567, and 330 μm sand, respectively. All of these observations suggest considerable deviations from CFT predictions.

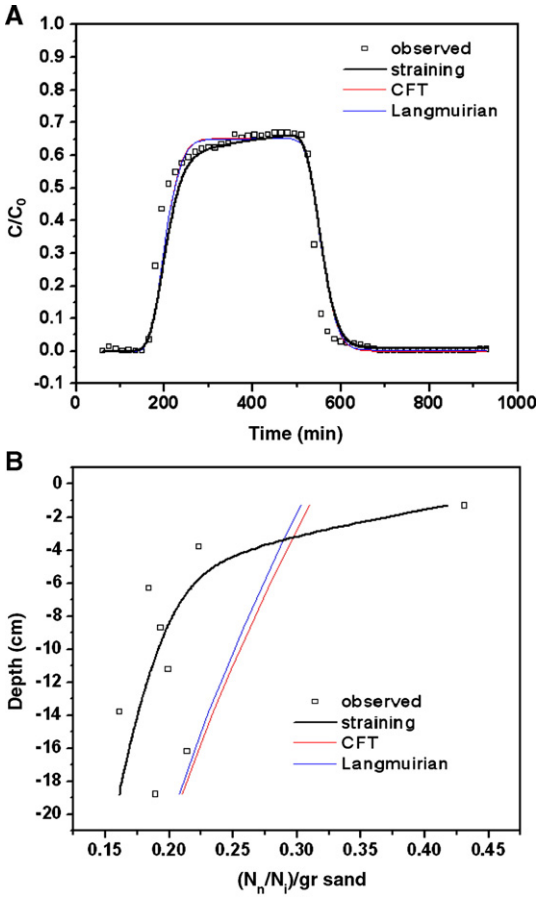

Fig. 3. Measured and fitted breakthrough curves (A) and retention profiles (B) for untreated *Rhodococcus rhodochrous* at 80% saturation and grain size of 567 μm. Fitted curves were obtained using the classical filtration theory (CFT) (red), Langmuirian blocking (blue), and straining (black) models.

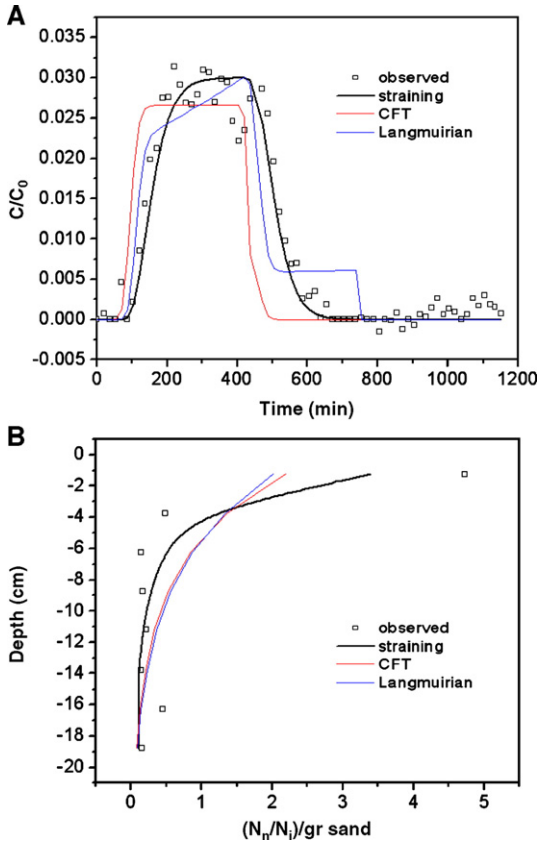

Fig. 4. Measured and fitted breakthrough curves (A) and retention profiles (B) for untreated *Rhodococcus rhodochrous* at 80% saturation and grain size of 330 μm. Fitted curves were obtained using the classical filtration theory (CFT) (red), Langmuirian blocking (blue), and straining (black) models.

Figs. 2–4 also present simulated bacteria transport behaviour in the 607, 567, and 330 μm sands, respectively, using the straining model (Eqs. (1) and (4)). Table 3 summarized fitted model parameters and statistical parameters for the goodness of fit. Table 1 includes the percentage of bacteria mass retained by attachment and straining processes as predicted by the straining model. Note in Figs. 2–4 and Table 3 that the straining model provide a good description of both breakthrough curves and deposition profiles. Table 1 indicates that straining was the dominant mechanism of bacteria deposition in all the sands, and that the percent mass retained by straining dramatically increases with decreasing sand size (9.7, 27.6, and 96.7% for the 607, 567, and 330 μm sands, respectively). This observation suggests that decreasing the pore size in the unsaturated systems significantly enhanced the straining. Bradford et al. (2002, 2003), Bradford and Bettahar (2006) similarly found that straining increased with decreasing sand size in saturated systems.

Fig. 5 shows a transverse slice of the packed column near the inlet for the transport experiment in the finest (330 μm) textured sand. The bacteria accumulation on the sand surface is visible, and the biomass appears to be filtered-out in the first sand centimetres after the injection point. In agreement with the modelling results, this is attributed to bacteria straining in the small pores and

Table 2
Fitted parameters of the CFT and Langmuirian blocking models for *untreated Rhodococcus rhodochrous*

Grain size	Coarse		Medium		Fine		Medium treated	
	Value	S.E. coeff.	Value	S.E. coeff.	Value	S.E. coeff.	Value	S.E. coeff.
Classical filtration theory								
k_a (min^{-1})	1.29E−03	22.7	2.96E−03	8.80E−09	2.20E+03	7.28E+04	2.20E−03	1.00E+03
R^2	0.98		0.96		0.7		0.98	
R^2 (btc*)	0.98		0.97		0.82		0.96	
R^2 (rp^+)	0.36		0.41		0.69		0.29	
Langmuirian blocking								
k_a (min^{-1})	2.40E−03	0.16	2.99E−03	2.01E−04	0.032	2.2	0.3E−2	0.21E−3
k_d (min^{-1})	9.10E−04	2.48E−03	2.55E−05	6.77E−05	1.88E−04	8.13E−04	0.47E−5	0.79E−4
s_{max}(Nn/Ni)/gr sand	0.159	9.12E−04	5.23E+03	1.03E+07	1.90E+01	3.85E−05	0.25	0.047
R^2	0.98		0.97		0.7		0.98	
R^2 (btc*)	0.98		0.96		0.84		0.80	
R^2 (rp^+)	0.37		0.11		0.05		0.80	

* Breakthrough curve, $^+$ retention profile.

at grain–grain junctions. In the finest sand, the straining was enhanced due to the higher ratio of the bacteria to pore diameter and by the aggregation behaviour of *Rhodococcus* due to its hydrophobic cell surface characteristics (Gargiulo et al., submitted for publication). Crist et al. (2005) visualized colloid transport processes in porous media. These authors found greater deposition of the hydrophobic colloids due to attractive hydrophobic forces between colloids that produced aggregates that were subsequently retained in the narrow passages between grains. Once deposited, these aggregates served as preferred sites for subsequent deposition of other hydrophobic colloids.

Table 1 indicates that straining accounted for more than 78% of the total deposited bacteria in the various sands, reaching 99.6% in the finest 330 μm sand. The influence of bacteria attachment in the experimental sands was confounded by straining which significantly lowers the aqueous bacteria concentration with transport depth that can subsequently attach to solid–water or air–water interfaces. Hence, a systematic trend in the measured attachment coefficients and the percent mass attached is not apparent in Table 1.

3.2. Role of surface macromolecules

To investigate the role of surface macromolecules on bacteria surface characteristics and deposition mechanisms in unsaturated systems, *Rhodococcus* was *treated* with α-*Chymotrypsin* enzyme to degrade the peptides bond of cell surface macromolecules. The MATH test results indicate that this treatment had a significant effect on the bacteria surface hydrophobicity. The percent hydrophobicity of treated cells was measured to be 21%. In contrast, untreated cells were previously reported by Gargiulo et al. (submitted for publication) to have a hydrophobicity of between 55–90%. A close relationship between bacteria surface hydrophobicity and protein content was established in other studies (Neu, 1996; Sanin et al., 2003). It has been reported that bacteria cell surface hydrophobicity is caused by nitrogen-rich groups, most notably protein (Yang et al., 1999; Ginn et al., 2002).

In the last decade, several papers have been published on the use of *Fourier- transform* infrared (FT-IR) spectroscopy as a means of rapidly identifying microorganisms (Naumann et al.,

Table 3
Attachment, detachment, and straining coefficients of the straining model fitted to the column experimental data for different grain sizes and treated and untreated *Rhodococcus rhodochrous* cells

Variable	Value	S.E. coeff.
Coarse sand (607 μm)		
s_{max}	0.04	0.0003
$k_a(min^{-1})$	0.0008	0.0003
$k_d(min^{-1})$	0.032	0.08
β	0.648	0.004
$k_{str}(min^{-1})$	0.017	0.002
R^2	0.99	
R^2 (btc*)	0.99	
R^2 (rp^+)	0.69	
Medium sand (567 μm)		
s_{max}	5.5	5.8
$k_a(min^{-1})$	0.003	4E−4
$k_d(min^{-1})$	2E−6	1E−4
β	1.25	0.27
$k_{str}(min^{-1})$	0.08	0.05
R^2	0.96	
R^2 (btc*)	0.94	
R^2 (rp^+)	0.91	
Fine sand (330 μm)		
s_{max}	19.17	5.3
$k_a(min^{-1})$	0.025	0.009
$k_d(min^{-1})$	0.06	0.02
β	0.37	1.17
$k_{str}(min^{-1})$	0.199	1.19
R^2	0.91	
R^2 (btc*)	0.96	
R^2 (rp^+)	0.99	
Medium sand (567 μm). Treated cells		
s_{max}	0.02	0.003
$k_a(min^{-1})$	0.001	4E−3
$k_d(min^{-1})$	0.0015	7E−4
β	0.88	0.02
$k_{str}(min^{-1})$	0.08	0.422
R^2	0.99	
R^2 (btc*)	0.95	
R^2 (rp^+)	0.98	

1991; Ngo-Thi et al., 2003; Erukhimovitch et al., 2005). IR spectrum can serve as a microorganism's fingerprint providing quantitative information about total biochemical composition of the cell wall components (Naumann et al., 1991). Using this technique it is possible to characterize the cell surface and to obtain important information about the bacteria surface chemical structure (Sharma et al., 2003; Flint et al., 2001). In this study, this technique was used to characterize the surface composition of *R. rhodochrous* cells before and after the treatment with α-*Chymotrypsin,* a proteolitic enzyme.

Fig. 6 provides the IR transmittance spectrum for treated and untreated *R. rhodochrous* cells. The bands between 3000 and 2800 nm are related to the alkyl-hydrocarbons groups, the so called

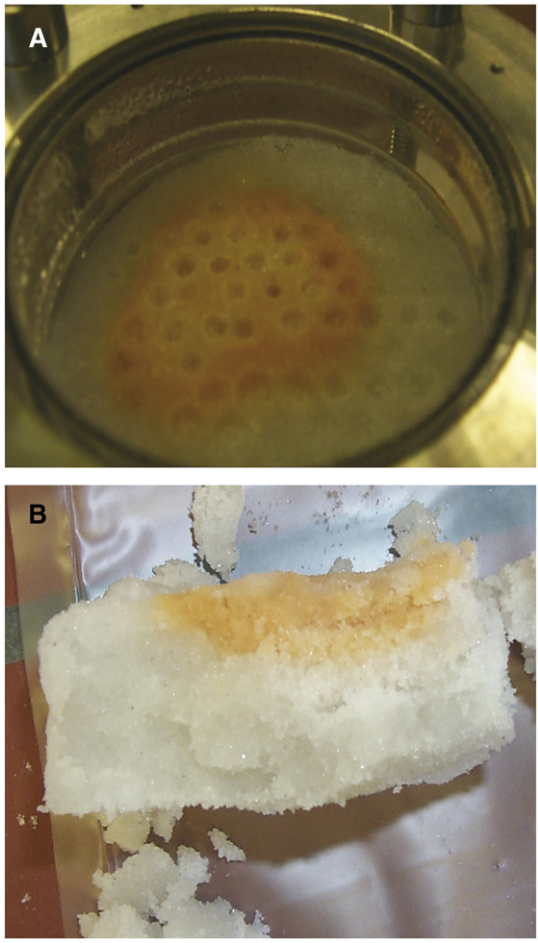

Fig. 5. Photos of the sand surface close to the injection point for the column experiment under unsaturated conditions (80%) with untreated *Rhodococcus rhodochrous* and the sand grain size of 330 μm. (A) Surface of the first sand layer. (B) Transverse cut of the first sand layer.

fatty acid region (Ngo-Thi et al., 2003). The bands at 2956, 2934 and 2875 nm characterize asymmetric CH_3 stretching, the asymmetric CH_2 stretching, and the symmetric CH_3 stretching, respectively. A protein region occurs between 1655 and 1546 nm (Dukor, 2001), and amide I and II bands can be identified. A very intense band between 1700 and 1600 nm indicates the presence of the C=O group. The shoulder at 1750 nm has been attributed to lipid C=O. The band at 1450 nm represents asymmetric CH_3 at the end of ethyl groups of proteins (Erukhimovitch et al., 2005). Fig. 6 indicates that the treatment of the bacteria surface with α-*Chymotrypsin* strongly affected the spectra. In comparison to the spectra of the untreated bacteria several of the detected peaks were diminished. For example, at 1450 and 1245 nm the bands for the treated bacteria completely disappeared (as mentioned above, this band was attributed to proteins), whereas the band at 1390 nm is still present. The band at 3071 nm is assigned to the symmetric stretching of the NH_2 group, and a strong decreasing was found for the treated cells. Decreases in these bands are expected with protease treatment in the area assigned to the alkyl-hydrocarbons groups and

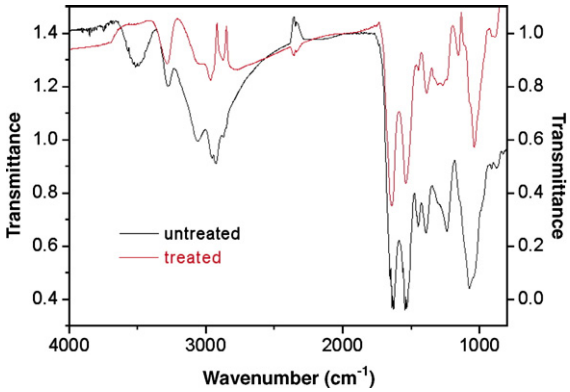

Fig. 6. Infrared analysis of *Rhodococcus rhodochrous* cells showing the difference between untreated cells and cells treated with α-*Chemotrypsin*.

proteins. A stronger decreasing in the band intensity at 2934 and 2875 nm compared with the decrease at 2956 nm was an indication that long alkyl chains have been removed. It is therefore reasonable to assume that hydrocarbon chains were associated with the protein structures that were removed. This finding may explain the decrease in hydrophobicity observed with the MATH test. Proteins are also hydrophobic molecules and their removal from the cell surface may have also had a role in the decreased hydrophobicity.

Hydrophobicity is an important parameter that influences bacteria attachment to surfaces (Rosenberg and Doyle, 1980; Van Loosdrecht et al., 1987, 1989). Flint et al. (2001) reported that a treatment with *Trypsin* or sodium dodecyl sulphate to remove cell surface proteins resulted in a 100-fold reduction in the number of bacteria cells that attached to a stainless steel surface. Caccavo (1999) demonstrated that surface proteins played a significant role in the attachment process, and that bacteria treated with proteolytic enzymes had less capability for adhesion. Consequently the presence of proteins, more than other surface macromolecules, acts to enhance bacteria attachment. Caccavo (1999) also reported on adhesion experiments using bacteria that were enzymatic and chemically treated to damage both the proteins and the lipo-polysaccharides on the bacteria surface. In most cases the treatment to damage the protein, led to a decrease in adhesion of bacteria. Walker et al. (2005) found a decrease in adhesion and hydrophobicity of *E.coli* during *mid-exponential* compared with the *stationary* phase. These observations were attributed to hydrophilic (acidic) proteins on the outer membrane of *E.coli* that decrease with the culture age, and consequently lead to a decrease in hydrophobicity and adhesion.

Fig. 7 shows the breakthrough curve for treated and untreated *R. rhodochrous* cells in 567 μm sand at a water saturation of 80%. The mean front of treated and untreated bacteria arrived at the same time, however, the peak effluent concentrations were different. For the untreated cells, the peak value of c/c_0 was 0.8, and for treated bacteria a lower value of 0.65 was observed. Fig. 8 shows a plot of the corresponding deposition profiles. As observed in the experiments using different sand sizes, the retention profile for the treated bacteria did not exhibit an exponential decrease with distance as predicted by classical filtration theory. The retention profiles for both treated and untreated cells were hyper-exponential and the deposition was enhanced in the sand adjacent to the column inlet. The relative number of treated and untreated bacteria in the sand adjacent to the column inlet had a very similar value, suggesting that the enzyme treatment of the

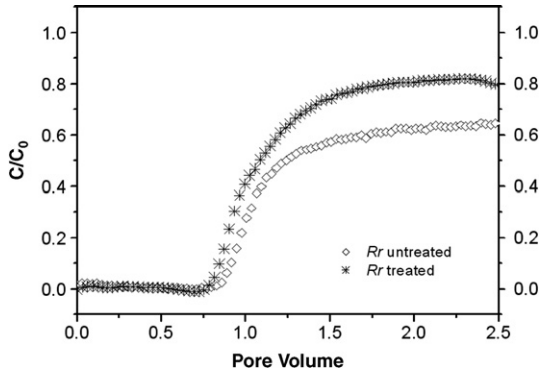

Fig. 7. *Rhodococcus rhodochrous* breakthrough curves for untreated cells and cells treated with α-*Chemotrypsin* in 567 μm sand and a water saturation of 80%.

bacteria did not significantly influence straining behaviour. The main difference in the deposition profile was measured with greater transport distances. In this region, the treated bacteria were retained to a lesser extent than untreated cells. This observation is attributed to a decrease in attachment as a result of the measured decrease in hydrophobicity.

The CFT, Langmuirian blocking, and straining models were used to characterize the transport data presented in Fig. 9A and B for the bacteria that was subject to treatment by α-*Chymotrypsin* enzyme. A summary of the fitted model and statistical parameters is provided in Tables 2 and 3. The CFT and Langmuirian models provided only an accurate description of the breakthrough curve, but the deposition profile was poorly characterized by these models. Conversely, the straining model could properly fit both effluent and deposition data. The straining model parameters for untreated and treated bacteria in 567 μm sand were subsequently compared to gain additional insight on the deposition mechanisms. The value of k_a for the treated bacteria was inferior to the untreated bacteria. This result demonstrates the importance of the proteins on the bacteria surface to promote attachment. Other researchers have also reported that interactions between the outer bacteria proteins and the solid surface play a dominant role in the microbial

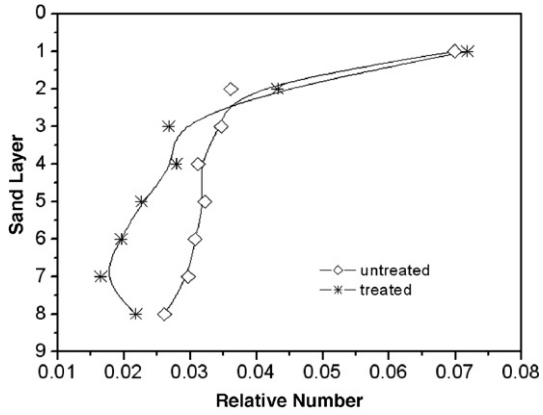

Fig. 8. *Rhodococcus rhodochrous* retention profiles for untreated cells and cells treated with α-*Chemotrypsin* in 567 μm sand and a water saturation of 80%.

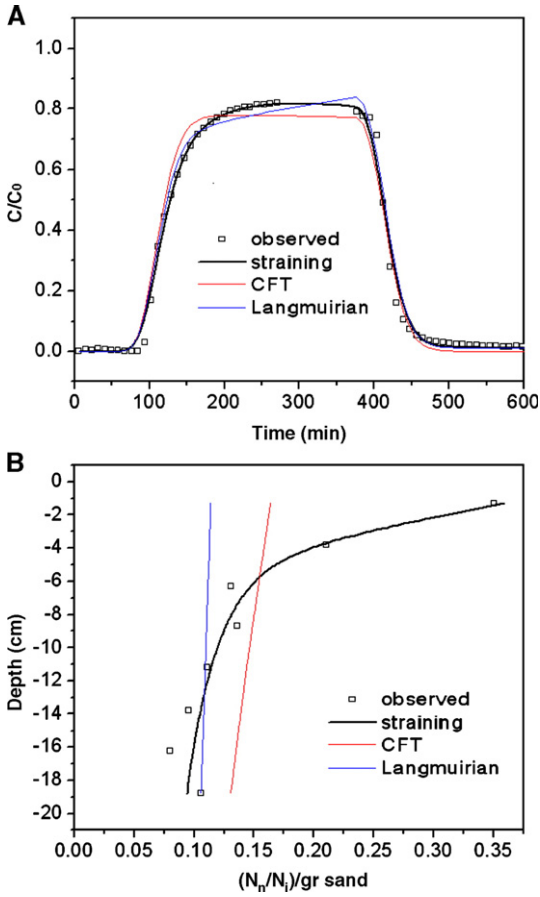

Fig. 9. *Rhodococcus rhodochrous* breakthrough curves (A) and retention profile (B) for cells treated with α-*Chymotrypsin* in 567 μm sand and a water saturation of 80%. Fitted curves were obtained using the Classical filtration theory (CFT) (red), Langmuirian blocking (blue), and straining (black) models.

adsorption processes (Norde et al., 1989; Sanin et al., 2003). The value of k_{str} was quite similar for treated and untreated bacteria, which demonstrated that bacteria treatment did not significantly influence straining, presumably because the cut proteins did not affect the bacteria size; i.e., only a macromolecular layer was removed from the cell surface.

4. Summary and conclusions

The goal of this work was to investigate the influence of grain size and bacteria surface macromolecules (in particular proteins) on unsaturated bacteria transport. A special focus was to quantify attachment and straining mechanisms of deposition. All transport experiments were conducted at a water saturation of 80% and using *R. rhodochrous*, a hydrophobic bacterium that has a tendency to form aggregates. Experimental effluent and deposition data were described using a mathematical model that accounts for reversible attachment, and time and depth-dependent straining. This modelling approach lumped processes of deposition on the solid–water

and air–water interfaces into a single attachment coefficient, and film and pore straining processes into a single straining coefficient. Bacteria transport through different sized sands (607, 567, and 330 μm) was directly related to median grain size. Decreasing the sand size resulted in a reduction in the effluent concentration and enhanced deposition close to the column inlet. For the considered sands, the deposition profile was not consistent with classical filtration theory predictions. The deposition profile did not decrease exponentially with distance, but rather was hyperexponential. Visual observations of the deposition profiles, and mathematical modelling results indicated that straining was the primary mechanism of deposition and accounted for 78–99.6% of the deposited bacteria. Aggregation of this bacterium strain undoubtedly enhanced the amount of straining deposition in these experimental systems.

Additional studies were conducted to investigate the role of surface macromolecules on bacteria transport. In this case, a proteolitic enzyme was used to cut the macromolecules from the bacteria surface. Changes in the surface properties of *R. rhodochrous* were assessed by measuring the hydrophobicity and the Fourier-transformed infrared spectrum of enzyme treated and untreated bacteria. The percent hydrophobicity of treated and untreated cells according to the MATH test was 21% and 55–90%, respectively. Measurement of the infrared spectrum also revealed distinct changes in the spectrum associated with removal of macromolecules due to this enzyme treatment. Comparison of transport data for enzyme treated and untreated bacteria in a given sand provided interesting information on the roles of proteins on deposition. Straining behaviour for treated and untreated bacteria was quite similar, suggesting that macromolecules do not play a dominant role in straining deposition. Conversely, enzymatic surface treatment significantly lowered the amount of attached cells throughout the column length and hence produced greater mobility.

References

Adamczyk, Z., Siwek, B., Zembala, M., Belouschek, P., 1994. Kinetics of localized adsorption of colloid particles. Advance in Colloid and Interace Science 48, 151–280.

Bolster, C.H., Mills, A.L., Hornberger, G.M., Herman, J.S., 2001. Effect of surface coatings, grain size, and ionic strength on the maximum attainable coverage of bacteria on sand surfaces. Journal of Contaminant Hydrology 50, 287–305.

Bradford, S.A., Bettahar, M., 2005. Straining, attachment, and detachment of cryptosporidium oocysts in saturated porous media. Journal of Environmental Quality 34, 469–478.

Bradford, S.A., Bettahar, M., 2006. Concentration dependent transport of colloids in saturated porous media. Journal of Contaminant Hydrology 82 (1–2), 99–117.

Bradford, S.A., Yates, S.R., Bettahar, M., Šimůnek, J., 2002. Physical factors affecting the transport and fate of colloids in saturated porous media. Water Resources Research 38 (12), 1327. doi:10.1029/2002WR001340.

Bradford, S.A., Šimůnek, J., Bettahar, M., van Genuchten, M.Th., Yates, S.R., 2003. Modeling colloid attachment, straining and exclusion in saturated porous media. Environmantal Science & Technology 37, 2242–2250.

Bradford, S.A., Šimůnek, J., Bettahar, M., van Genuchten, M.Th., Yates, S.R., 2006. Significance of straining in colloid deposition: evidence and implications. Water Resources Research 42 (W12S15), 16. doi:10.1029/2005WR004791.

Caccavo Jr., F., 1999. Protein-mediated adhesion of the dissimilatory Fe (III)-reducing bacterium *Shewanella alga* BrY to hydrous ferric oxide. Applied and Environmental Microbiology 65, 5017–5022.

Crist, J.T., Zevi, Y., McCarthy, J.F., Throop, J.A., Steenhuis, T.S., 2005. Transport and retention mechanisms of colloids in partially saturated porous media. Vadose Zone Journal 4, 184–195.

DeFlaun, M.F., Murray, C.J., Holben, W., Scheibe, T., Mills, A., Ginn, T., Griffin, T., Majer, E., Wilson, J.L., 1997. Preliminary observations on bacterial transport in a coastal plan aquifer. FEMS Microbiology Reviews 20, 473–487.

Dukor, R.K., 2001. Handbook of Vibrational Spectroscopy. Wiley, Chichester, UK, pp. 3335–3360.

Erukhimovitch, V., Pavlov, V., Talyshinsky, M., Souprun, Y., Huleihel, M., 2005. FTIR microscopy as a method for identification of bacterial and fungal infections. Journal of Pharmaceutical and Biomedical Analysis 37, 1105–1108.

Flint, S., Palmer, J., Bloemen, K., Brooks, J., Crawford, R., 2001. The growth of *Bacillus stearothermophilus* on stainless steel. Journal of Applied Microbiology 90, 151–157.

Fontes, D.E., Mills, A.L., Hornberger, G.M., Herman, J.S., 1991. Physical and chemical factors influencing transport of microorganisms through porous media. Applied and Environmental Microbiology 57, 2473–2481.

Foppen, J.W.A., Mporokoso, A., Schijven, J.F., 2004. Determining straining of *Escherichia coli* from breakthrough curves. Journal of Contaminant Hydrology 76, 191–210.

Gargiulo, G., Bradford, S., Šimůnek, J., Ustohal, P., Vereecken, H., Klumpp, E., (submitted for publication) Bacteria transport and deposition under unsaturated conditions: the role of water content and bacteria surface hydrophobicity. Submitted to Applied and Environmental Microbiology.

Ginn, T.R., Wood, B.D., Nelson, K.E., Scheibe, T.D., Murphy, E.M., Clement, T.P., 2002. Processes in microbial transport in the natural subsurface. Advances in Water Resources 25, 1017–1042.

Grasso, D., Smets, B.F., Strevett, K.A., Machinist, B.D., VanOss, C.J., Giese, R.F., Wu, W., 1996. Impact of physiological state on surface thermodynamics and adhesion of *Pseudomonas aeruginosa*. Environmental Science & Technology 30, 3604–3608.

Jewett, D.G., Logan, B.E., Arnold, R.G., Bales, R.C., 1998. Transport of *Pseudomonas fluorescens* strain P17 through quartz sand columns as a function of water content. Journal of Contaminant Hydrology 36, 73–89.

Johnson, P.R., Elimelech, M., 1995. Dynamics of colloid deposition in porous media: blocking based on random sequential adsorption. Langmuir 11, 801–812.

Johnson, W.P., Tong, M., Li, X., 2005. Colloid deposition in environmental porous media: deviation from existing theory is the norm; not the exception. EOS 86 (18), 179–180.

Kästner, M. 1989. Anreicherung und Isolierung von Chlorkohlenwasserstoffe abbauenden Mikroorganismen unter verschiedenen physiologischen Bedingungen -Abbaukinetiken und Test auf technische Nutzbarkeit zur Sanierung kontaminierter Grundwässer. *Dissertation an der Technischen Universität Braunschweig*.

Li, X., Scheibe, T.D., Johnson, W.P., 2004. Apparent decreases in colloid deposition rate coefficient with distance of transport under unfavorable deposition conditions: a general phenomenon. Environmantal Science & Technology 38 (21), 5616–5625.

McDowell-Boyer, L.M., Hunt, J.R., Sitar, N., 1986. Particle transport through porous media. Water Resources Research 22, 1901–1921.

Naumann, D., Helm, D., 1991. H. Labischinski, microbiological characterizations by FT-IR-spectroscopy. Nature 351, 81–82.

Neu, T.R., 1996. Significance of bacteria surface active compounds in interactions of bacteria with interfaces. Microbiological Reviews 60, 151–166.

Ngo-Thi, N.A., Kirschner, C., Naumann, D., 2003. Characterization and identification of microorganisms by FT-IR microspectrometry. Journal of Molecular Structure 661–662 (16), 371–380.

Norde, W., Lyklema, J., 1989. Protein adsorption and bacterial adhesion to solid surfaces: a colloid-chemical approach. Colloids and Surfaces 38 (1–3), 1–13.

Powelson, D.K., Mills, A.L., 1996. Bacterial enrichment at the gas water interface. Applied and Environmental Microbiology 62, 2593–2597.

Reynolds, K.A., 2004. Groundwater vulnerability to microbial contamination. Water Conditioning & Purification 56, 28–30.

Rosenberg, M., Doyle, R.J., 1980. Adherence of bacteria to hydrocarbon. FEMS Microbology Letters 9, 29–33.

Salerno, M.B., Logan, B.E., Velegol, D., 2004. Importance of molecular details in predicting bacterial adhesion to hydrophobic surfaces. Langmuir 20, 10625–10629.

Sanin, S.L., Sanin, F.D., Bryers, J.D., 2003. Effect of starvation on the adhesive properties of xenobiotic degrading bacteria. Process Biochemistry 38, 909–914.

Scandura, J.E., Sobsey, M.D., 1997. Viral and bacterial contamination of groundwater from on-site sewage treatment systems. Water Science Technology 35 (11–12), 141–146.

Schaefer, A., Ustohal, P., Harms, H., Stauffer, F., Dracos, T., Zehnder, A.J.B., 1998. Transport of bacteria in unsaturated porous media. Journal of Contaminant Hydrology 33, 149–169.

Schijven, J., Šimůnek, J., 2002. Kinetic modeling of virus transport at field scale. Journal of Contaminat Hydrology 55 (1–2), 113–135.

Sharma, P.K., Das, A., Hanumantha Rao, K., Forssbe, K.S.E., 2003. Surface characterization of *Acidithiobacillus ferrooxidans* cells grown under different conditions. Hydrometallurgy 71, 285–292.

Šimůnek, J., van Genuchten, M.Th., Šejna, M., 2005. The HYDRUS-1D software package for simulating the one-dimensional movement of water, heat, and multiple solutes in variably-saturated media. Version 3.0, *HYDRUS Software Series 1*, Department of Environmental Sciences, University of California Riverside, Riverside, CA. 270 pp.

Tufenkji, N., Elimelech, M., 2004. Deviation from the classical colloid filtration theory in the presence of repulsive DLVO interactions. Langmuir 20, 10818–10828.

Tufenkji, N., Elimelech, M., 2005a. Breakdown of colloid filtration theory: role of secondary energy minimum and surface charge heterogeneities. Langmuir 21, 841–852.

Tufenkji, N., Elimelech, M., 2005b. Spatial distributions of cryptosporidium oocysts in porous media: evidence for dual mode deposition. Environmantal Science & Technology 39, 3620–3629.

Tufenkji, N., Redman, J.A., Elimelech, M., 2003. Interpreting deposition patterns of microbial particles in laboratory-scale column experiments. Environmantal Science & Technology 37, 616–623.

Tufenkji, N., Miller, G.F., Ryan, J.N., Harvey, R.W., Elimelech, M., 2004. Transport of cryptosporidium oocysts in porous media: role of straining and physicochemical filtration. Environmantal Science & Technology 38, 5932–5938.

Yang, J., Bos, R., Belder, G.F., Engel, J., Busscher, H.J., 1999. Deposition of oral bacteria and polystyrene particles to quartz and dental enamel in a parallel plate and stagnation point flow chamber. Journal of Colloid and Interface Science 220, 410–418.

Van Loosdrecht, M.C.M., Lyklema, J., Norde, W., Schraa, G., Zehnder, A.J.B., 1987. The role of bacterial cell wall hydrophobicity in cell attachment. Applied and Environmental Microbiology 53, 1893–1897.

Van Loosdrecht, M.C.M., Lyklema, J., Norde, W., Zehnder, A.J.B., 1989. Bacterial adhesion: a physicochemical approach. Microbial Ecology 17, 1–15.

Walker, S.L., Hill, J., Redman, J.A., Elimelech, M., 2005. The influence of growth phase on adhesion kinetics of *Escherichia coli* D21g. Applied and Environmental Microbiology 71, 3093–3099.

Wan, J., Wilson, J.L., Kieft, T.L., 1994. Influence of the gas water interface on transport of microorganisms through unsaturated porous media. Applied and Environmental Microbiology 60, 509–516.